Title

Dendritic cell immunotherapy induces anti-tumor effect in a transgenic mouse model of pancreatic ductal adenocarcinoma.

Permalink

https://escholarship.org/uc/item/99t5d2md

Journal

American Journal of Cancer Research, 9(11)

ISSN

2156-6976

Authors

Yang, Jia
Hu, Su
Shangguan, Junjie
et al.

Publication Date

2019

Peer reviewed

Original Article
Dendritic cell immunotherapy induces anti-tumor effect in a transgenic mouse model of pancreatic ductal adenocarcinoma

Jia Yang[1*], Su Hu[1,2*], Junjie Shangguan[1], Aydin Eresen[1], Yu Li[1,3], Liang Pan[1,4], Quanhong Ma[1], Yuri Velichko[1,5], Jian Wang[6], Chunhong Hu[2], Vahid Yaghmai[1,5], Zhuoli Zhang[1,5]

[1]Department of Radiology, Feinberg School of Medicine, Northwestern University, Chicago, IL, USA; [2]Department of Radiology, The First Affiliated Hospital of Soochow University, Suzhou, Jiangsu, China; [3]Department of General Surgery, The Affiliated Hospital of Qingdao University, Qingdao, Shandong, China; [4]Department of Radiology, The Third Affiliated Hospital of Soochow University, Changzhou, Jiangsu, China; [5]Robert H. Lurie Comprehensive Cancer Center, Northwestern University, Chicago, IL, USA; [6]Department of Radiology, Southwest Hospital, Chongqing, China. *Equal contributors.

Abstract: The promise of dendritic cell (DC)-based immunotherapy has been established by two decades of translational research. However, long-term benefits of DC vaccination are reported in only scattered patients with pancreatic ductal adenocarcinoma (PDAC). Here we optimize DC vaccination and evaluate its safety and antitumor efficacy in the genetically engineered PDAC model (*Kras$^{LSL-G12D}$ p53$^{LSL-R172H}$ Pdx-1-Cre* (KPC mice)). KPC transgenic mice and orthotopic models using KPC cell lines were treated with DC vaccine via an intraperitoneal route. Tumor growth and microenvironment were dynamically monitored by magnetic resonance imaging (MRI). Histological analysis and flow cytometry were used to evaluate tumor-directed T cell immunity of these mice. DC vaccine via intraperitoneal injection suppressed tumor progression (P = 0.030) and significantly prolonged survival time (P = 0.028) in KPC mice. Vaccinated KPC mice displayed an increased antitumor T cell response indicated by a higher IFN-γ production (P = 0.016) and tumor-specific cytotoxicity (P = 0.027). Particularly, the mean apparent diffusion coefficient (ADC) values of KPC tumor calculated from diffusion weighted MRI (DW-MRI) were significantly higher in DC vaccine group than that in control group (P < 0.001). More interestingly, we observed that ADC positively correlated with fibrosis in KPC tumor (R^2 = 0.463, P = 0.015). Our study demonstrated that the immunization with our improved DC vaccine can elicit a strong tumor-specific immune response and tumor suppression in PDAC.

Keywords: Pancreatic ductal adenocarcinoma, DC-based immunotherapy, magnetic resonance imaging

Introduction

Currently, the 5-year survival rate of patients with pancreatic ductal adenocarcinoma (PDAC) is less than 5% due to late diagnosis and early metastases [1]. Surgical resection is the only potentially curative option, but only 10-20% of PDAC patients are eligible for surgery [2]. Even in patients with potentially operable tumor, 5-year overall survival is only about 20-25% [3].

Dendritic cells (DCs), which are professional antigen-presenting cells, play a pivotal role in the initiation of immune responses. DCs have a superior ability to transport and cross-present tumor associated antigens (TAA) to CD8^{+} T cells in draining lymph nodes (dLNs) [4], providing a rationale for their utilization as cancer vaccines. In recent years, *ex vivo* DCs pulsed with TAA were used as therapeutic vaccines against human cancers including PDAC [5, 6]. Despite years of effort, clinical responses were limited [7, 8]. There is a consensus that DC vaccines have not yet successfully and fully reached their potential. Additional studies are necessary to further explore the potential of DC vaccines. Efficient delivery of antigens into DCs, sufficient antigen-loaded DCs migration to dLNs, and strong induction of cytotoxic T lymphocytes (CTLs) mediated immune responses

are essential requirements for DC-based cancer immunotherapy [9]. Another consideration in DC-based cancer immunotherapy is the administration method [10]. The route of administration must allow efficient DC vaccines to reach the dLNs to prime naïve T-cell differentiation. However, a standardized method for DC vaccine delivery has not been established for both preclinical and clinical applications. Several administration routes, including intravenous [11], intranodal [12], subcutaneous [13], or intratumoral [14], have been used in clinical trials, but the therapeutic responses were not durable. A promising method is the intraperitoneal (i.p.) route, which allows increased DC-vaccine dosage on delivery and thus increased numbers of DCs migrating to lymph nodes (LNs) [15], particularly LNs in the abdomen. Our previous studies have compared the i.p. injection with footpad injection and show that the i.p. injection improves the efficiency of DC-based cancer vaccine [15-17]. Therefore, i.p. injection may be the most efficient injection route for the abdominal tumors.

Magnetic resonance imaging (MRI) is a well-established tool for noninvasively monitoring pancreatic tumor burden for both disease progression and treatment response due to its superior soft tissue contrast [18, 19], and also does not lead to exposure to ionizing radiation. Anatomic T2-weighted (T2W) and T1-weighted (T1W) MRI has been extensively used to identify the pancreatic tumors [20, 21]. Diffusion-weighted magnetic resonance imaging (DW-MRI) is a technique that can evaluate cellular structures in biological media and may be a powerful tool for differentiating PDAC from other pancreatic lesions [22, 23]. Furthermore, prior studies have reported that a low apparent diffusion coefficient (ADC) value calculated from DW-MRI is positively correlated with a poor response to chemotherapy in pancreatic cancer [24-26]. However, there are no standard non-invasive imaging methods to assess immunotherapy response and predict the prognosis in PDAC to date.

In this study, we used a transgenic mouse model of PDAC, $Kras^{G12D}$ $p53^{R172H}$ $Pdx1$-Cre (KPC) mice, to test the safety, feasibility, and antitumor efficacy (including overall survival) of DC vaccination using i.p. administration. We dynamically monitored the treatment efficacy by MRI tracking of tumor size and ADC values. We sought to further explore efficacious measures related to prognosis and investigate whether this relationship can be easily translated to clinical practice.

Materials and methods

Mice

All the animal protocols were reviewed and approved by the Institutional Animal Care and Use Committee of the Northwestern University. The generation and characterization of the KPC mice have been previously described in detail [27]. The mouse strains $p53^{LSL-R270H}$ (strain number 01XM3), $Kras^{LSL-G12D}$ (strain number 01XJ6), and $Pdx1$-cre (strain number 01XL5) were purchased from the Jackson Laboratory. 6-8 weeks old female C57BL/6 mice (Charles River, Wilmington, MA) were used to derive bone marrow-derived dendritic cells (BDMC).

Cell lines

KPC cells were derived from a spontaneous tumor in a 6-month-old KPC mouse and used for the cellular studies and growing orthotopic tumors in mice. Cells were cultured on collagen-coated plastic for < 12 passages. A murine PDAC cell line Pan02 cell line was purchased from ATCC. Both cell lines were cultured in complete RPMI 1640 medium containing 10% FBS, 100 U/mL penicillin, 100 μg/mL streptomycin, and 2 mM L-glutamine.

Generation of mature DCs

DCs were derived from bone marrow progenitor cells as described [28]. Briefly, bone marrow cells were harvested from the femurs of 6-8 weeks old C57BL/6 female mice and cultured in complete RPMI1640 containing mouse recombinant GM-CSF (10 ng/ml) and IL-4 (1 ng/ml) (both Invivogen, San Diego, CA) for 8 days in petri dish. Medium was refreshed on day 3 and day 6. On day 8, immature DCs were harvested by collecting non-adherent cells and then immediately pulsed by incubation with KPC tumor cell lysates in the presence of 100 ng/ml IFN-γ and 250 ng/ml LPS - E. coli 0111:B4 (both from Invivogen, San Diego, CA) as described previously [15]. KPC lysates were generated by collecting and resuspending KPC

tumor cells at 1×10^6 cells/ml in PBS, followed by irradiation with UV for 20 minutes (0.75 J/cm^2) and 24 h incubation.

Orthotopic KPC tumor implantation

Female C57BL/6 mice aged 8-10 weeks were used for establishing orthotopic PDAC models. 5×10^4 viable KPC cells (< 12 passages) suspended in a 3:1 PBS to Matrigel (Sigma-Aldrich, St Louis, MO) solution were directly injected into the pancreas for orthotopic tumor induction. Cohorts of mice were randomized into different treatment groups at 4-5 days following tumor inoculation.

Monitoring of tumor growth and therapy

At 3-month-old age, genotyped KPC genetic model of PDAC were monitored for the development of tumor by MRI every two weeks. KPC transgenic mice were enrolled when the longest tumor diameter reached 0.2-0.5 cm in MRI. Orthotopic KPC mice were enrolled after 5 days of tumor inoculation. Mice then received 3×10^6 DCs pulsed with irradiated KPC cell lysates by i.p. injection on days 1, 8, and 15 after enrollment while the control mice did not receive any treatment. Survival events were scored when mice displayed > 15% loss of body weight, > 1.8 cm tumor diameter, decreased mobility, extreme lethargy, or absolute survival event. All enrolled mice were weighed and monitored for signs of distress regularly. MRI was used to monitor tumor size of KPC mice. MRI studies were conducted as described previously [29]. KPC mice were anesthetized by inhalation of 1-2% isoflurane in air/O$_2$ (75/25% vol/vol, 2 L/min). Experiments were performed in a 7.0T small-animal MRI scanner with a commercial mouse coil (ClinScan, Bruker Biospin). The pancreas was localized using respiratory-gated coronal and axial T2-weighted fast spin-echo images (Turbo Spin Echo (TSE); Repetition time (TR): 1600 ms; Echo time (TE): 37 ms; slice thickness (ST): 1.0 mm; flip angle (FA): 180°; field of view (FOV): 36 × 28 mm^2). The MRI sequences and parameters were as follows: (a) axial T2-weighted imaging (T2WI): TSE; TR: due to respiratory gating approx. 2100 ms; TE: 40 ms; ST: 0.5 mm; FA: 180°; FOV: 21 × 30 mm^2; (b) coronal T2W images: TSE; TR: due to respiratory gating approx. 2100 ms; TE: 40 ms; ST: 0.5 mm; FA: 180; FOV: 40 × 30 mm^2; (c) axial diffusion-weighted imaging (DW-MRI): Echo Pla-

nar Imaging (EPI); TR: due to respiratory gating approx. 2700 ms; TE: 40 ms; ST: 1 mm; FA: 90°; FOV: 24 × 30 mm^2; b value = 0, and 800 s/mm^2. DW-MRI was performed in 3 orthogonal directions of the diffusion gradients. ITK-SNAP was used for volume calculations and three-dimensional (3D) reconstructions. MATLAB R2018a (Mathworks, Natick, MA) and ImageJ 1.52a (http://imagej.nih.gov/ij) were used for additional image processing and ADC calculations.

In vivo migration assays

Mice were i.p. injected with 3×10^6 DCs dyed by CellTrace CFSE (Thermo Fisher Scientific, Waltham, MA). Draining (pancreas) lymph nodes were harvested at 6 h post injections and digested into single-cell suspensions. CFSE$^+$ DCs migrating from the site of injection to the pancreatic LN and spleen were quantified in flow cytometric analysis. NdLN from the same treated animals and spleen from the untreated mice were used as control.

In vivo specific cytotoxicity assays

Splenocytes from 8 to 10 weeks old C57BL/6 mice were seeded in the 24-well plates (5 × 10^6 per well) and co-cultured with UV-KPC cells (2 × 10^5 per well) for 4 h. The remaining splenocytes were left unpulsed. Pulsed splenocytes were labeled with CFSE to generate CFSE^{high} splenocytes, and unpulsed splenocytes were labeled with 20 × diluted CFSE to generate CFSE^{low} splenocytes. The unpulsed CFSE^{low} and pulsed CFSE^{high} labeled splenocytes were mixed at a 1:1 ratio in PBS to a final concentration of 5×10^7 cells per ml. 100 μl of the cell mixture was injected intravenously into immunized mice (3-5 d after treatment), untreated tumor-bearing mice, and 2 naive (non-tumor bearing) mice. 16 h after injection, spleens were collected for flow cytometry analysis. Percentage of specific lysis was calculated according to % specific lysis = (1 - (ratio CFSE^{high}:CFSE^{low} in experimental mouse/average ratio CFSE^{high}:CFSE^{low} in naive mice)) × 100.

Splenocytes proliferation assays

Four days after the last immunization, splenocytes harvested from two groups were seeded in the 96-well plate (5 × 10^5 per well) and restimulated with UV-KPC cells (2 × 10^4 per well)

for 24 h. Splenocytes proliferation was measured using the CCK-8 kit (DOJINDO, Japan) analysis. OD values at 450 nm were recorded by a microplate reader.

Flow cytometry analysis

Single cell suspension was obtained from KPC mice spleen. Activated BMDCs and *in vitro* culture cells were labeled with fluorochrome-conjugated mAbs (From BioLegend) after neutralization of unspecific binding with FcR blocker (BD Biosciences, San Jose, CA). Data was acquired on a BD LSRFortessa™ cell analyzer (San Jose, CA) and analyzed using the FlowJo software (TreeStar Inc, Ashland, OR, USA).

Enzyme-linked immunosorbent assay (ELISA)

IFN-γ expression was detected by ELISA. The concentrations of IFN-γ in mice serum collected after 4 days of the last treatment and cell culture supernatants were determined using mouse IFN-γ kit (R&D bioscience, Minneapolis, MN) according to the manufacturer's protocols. The absorbance was measured at 450 nm with a microplate reader.

Histology analysis

Tissues were fixed in 10% formalin and embedded in paraffin. 5-μm sections of pancreatic tissues were selected for H&E and Masson's Trichrome stains according to manufacturer's instructions. Whole-tissue slide scans were performed on TissueFAXS system. Image analysis was performed using Image J software.

Immunohistochemistry (IHC)

Tissues were fixed in 10% formalin and embedded in paraffin. Then 5-μm-thick sections were deparaffinized in xylene, rehydrated in graded ethanol, and subjected to antigen retrieval by steam heating in Citra antigen retrieval solution (Vector, Burlingame, CA). After blocking for 1 h at room temperature in blocking buffer (5% goat serum, 2.5% BSA in 1 × PBS), slides were incubated overnight in a humidified chamber at 4°C with anti-mouse CK19 (kindly provided by the Developmental Studies Hybridoma Bank), rabbit monoclonal anti-Ki67 (Clone SP6, Invitrogen), and rat monoclonal anti-mouse CD8 (Clone 4SM15, Invitrogen). Immunostaining was detected using 3,3'-diaminobenzidine

(DAB) (Vector, Burlingame, CA). Quantification was performed using ImageJ software at a high field magnification.

Statistical analysis

The values are reported as mean and the standard error of the mean (SEM). Statistical significance was either assessed via an unpaired two-tailed Student's *t*-test or 2-way ANOVA with Bonferroni post-test. The overall survival was assessed using the Kaplan-Meier method, and the survival difference between groups was compared using the log-rank test. $P < 0.05$ was considered significant. Statistical analysis was performed using GraphPad Prism software version 7.0 (La Jolla, CA, USA).

Results

Vaccination with KPC pulsed DCs resulted in an antitumor T-cell response in KPC mice

Murine DCs were generated from the bone marrow of C57BL/6 mice and matured by incubation with LPS, IFN-γ, and UV-KPC cells. Their maturation status was verified by surface marker staining (**Figure 1A**), indicating that pulsing of DCs with irradiated necrotic cells does not impact DC maturation and activity.

The entry of antigen-bearing DCs into dLNs is known to be important for their ability to effectively activate tumor-specific CTLs [30]. To verify whether pulsed DCs can effectively traffic to the dLNs, C57BL/6 mice were i.p. injected with CFSE-dyed DCs. CFSE-labeled CD11c DCs were observed in the dLNs and spleen 12 hours after injection (**Figure 1B**). As a control for the specificity of the migration, ndLN were also obtained from the inguinal LN of the same mice and the spleen of untreated mice, where no CFSE positive cells were detected (**Figure 1B**).

Then, to evaluate the *in vivo* specific cytotoxicity induced by i.p. administration of DC vaccine, the unpulsed CFSE^{low}- and pulsed CFSE^{high}-labeled splenocytes were mixed at a 1:1 ratio, and intravenously injected into the tumor-bearing mice. Splenocytes were harvested for flow cytometry analysis 12 h after injection. Strikingly, splenocytes from DC-vaccinated mice lysed ~45% target KPC cells, while the control group only lysed ~16% (**Figure 1C**). Furthermore, the tumor infiltrating CD8$^+$ T cells were significantly
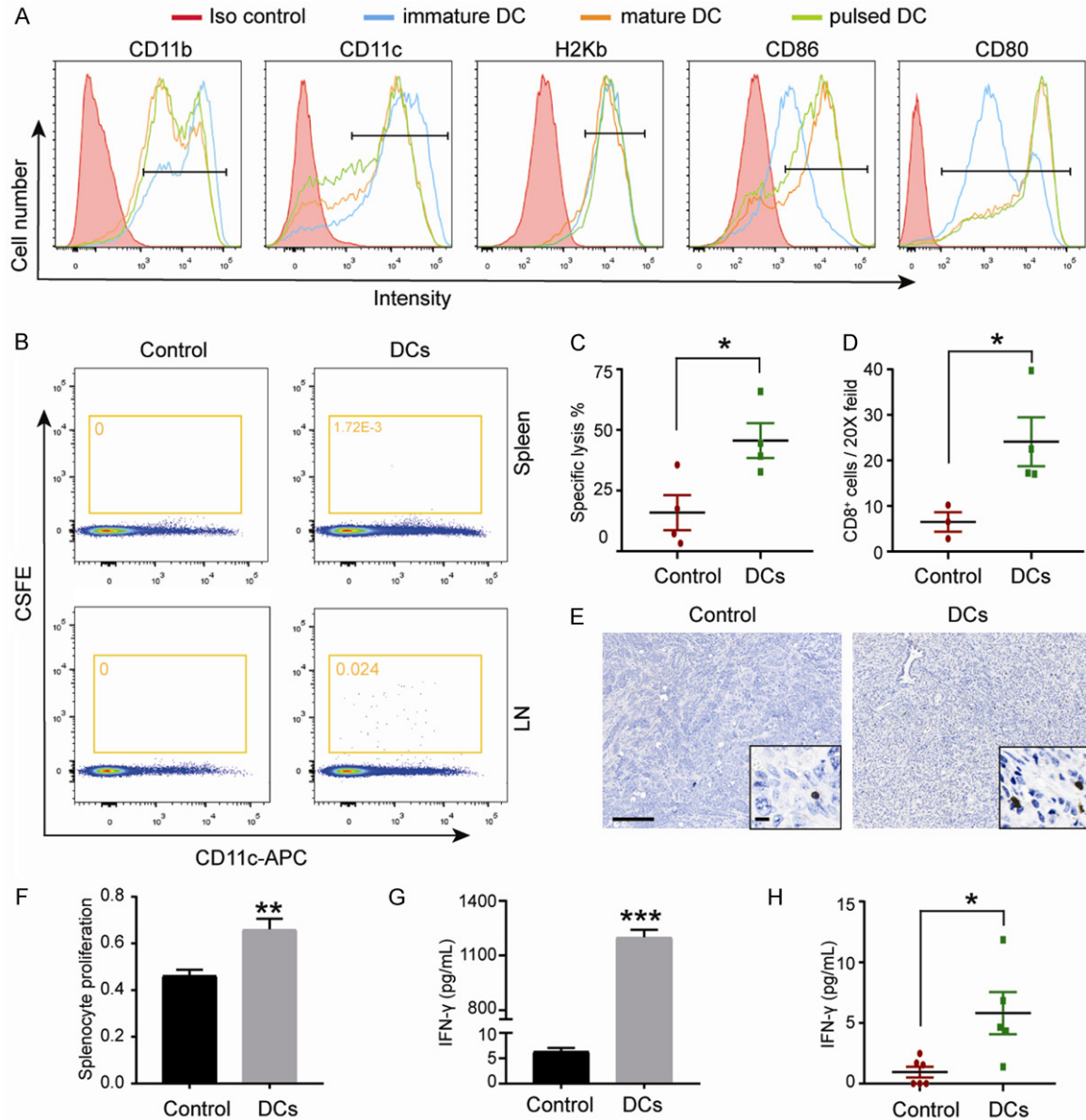
Figure 1. Vaccination with KPC pulsed DCs resulted an antitumor T-cell response in KPC mice. (A) Flow cytometry for analyzing levels of surface proteins in immature dendritic cells (DC), mature DC or KPC loaded DC. A representative example of three independent experiments is shown. (B) Representative scatter plots of migrated DCs in the spleen and lymph node are shown. For DCs group, the spleen and pancreatic LN from the DCs treated mice were used. For control group, ndLN (inguinal) from the DCs treated mice and the spleen from untreated mice were used. (Representative experiment, n = 3). (C) *In vivo* CTLs assay. Naïve splenocytes were labeled with 20 × diluted CFSE (left peaks) or with CFSE (right peaks) and pulsed with UV-KPC cells, as target cells. Target cells at 5×10^6 were injected intravenously into the recipient mice 3-5 days after treatment. Splenocytes were collected from the recipient mice for detection of CFSE-labeled cells by flow cytometry at 16 hours. Quantitation of specific lysis are shown (n = 4). (D) Representative images of tumor infiltrating CD8+ T cells. Scale bars represent 200 μm (inset, 25 μm) and (E) quantification are shown (n = 4). (F) Results of the proliferation of splenocytes. Spleen cells obtained from treated mice were co-cultured with UV-KPC, and the cell proliferation was evaluated by a CCK-8 kit assay. (G) Measurement of IFN-γ in serum from treated mice on day 4 after the last treatment (n = 5-6). (H) The production of IFN-γ in the culture supernatants. Splenocytes of surviving mice (DC treatment group and control group), were isolated when the mice were sacrificed and cultured in the presence of KPC tumor cells. Data were combined from three experiments. *$P < 0.05$, **$P < 0.001$. Data are expressed as the mean ± SEM.

increased in treated group than in control group (**Figure 1D**, **1E**). These findings together suggest that i.p. administration of pulsed DCs were efficient in inducing CTL response specifically

against KPC cells. More importantly, DC vaccine treatment remarkably promoted the proliferation of KPC-specific splenocytes (**Figure 1F**) and triggered higher levels of IFN-γ in the culture supernatants (**Figure 1G**) compared with the control group when the splenocytes were re-stimulated with UV-KPC cells. Additionally, measurement of cytokines associated with the inflammatory response in mouse blood showed a significantly increased serum level of IFN-γ (**Figure 1H**). An independent experiment that was conducted to evaluate the effects of DCs without incubation with irradiated cancer cells on PDAC tumor growth. The equal amount of DCs were used to treat the PADC mice. The results showed no significant difference of PDAC tumor growth rate between the DCs without incubation with irradiated cancer cells and control group (P = 0.916) (Figure S1), suggesting that the injection of a large number of DCs did not induce antitumor immune response itself. Taken together, these results demonstrate that treatment with KPC-pulsed DCs via i.p. administration induced an effective antitumor immune response in PDAC mice.

DC vaccination inhibits tumor growth in PDAC mice models

To further assess the therapeutic efficacy of i.p. administration of KPC pulsed DCs on PDAC progression *in vivo*, we treated the KPC genetic model of PDAC when tumors are detectable on MRI (0.2-0.5 cm in the longest diameter) (**Figure 2A**). DC vaccine treatment significantly delayed tumor growth compared with control group (**Figure 2B**, **2D**). To further confirm these results and eliminate effects of different tumor stages, orthotopic KPC tumors were established. In according with our results from KPC genetic model of PDAC, DC vaccine treatment of mice bearing orthotopically implanted PDAC tumors via i.p. injection suppressed tumor growth (**Figure 2C**, **2E**). These results taken together suggest that i.p. administration of pulsed DC vaccine can potently elicit specific anti-tumor effects in PDAC mice.

Injection of KPC pulsed DCs delays the development of PDAC in KPC mice

Histological analysis of the sample tissues showed the presence of tumors with a desmoplastic reaction and the absence of normal-looking tissue in the control group. In comparison, DC vaccine treated KPC mice had tumors with desmoplastic reaction with the presence of some acinar cells (**Figure 3A**). CK19 (ductal marker) staining showed the presence of a diffuse cytoplasmic staining in tumor cells in the pancreas (**Figure 3A**, **3B**). Of note, the area of CK19 positive cells was larger in the DC vaccine treatment group than in control group, again corroborating that DC vaccination lead to a less extensive neoplastic transformation. Pancreatic cell proliferation assessed by Ki67 immunostaining was 2-fold lower in DC vaccine treatment group than in the control group (**Figure 3A**, **3C**). Taken together, these data provide additional evidence that DC vaccine can effectively suppress PDAC tumor development in KPC mice.

DC vaccine decreases tumor fibrosis in KPC mice

To determine the impact of DC vaccine treatment on the formation of the otherwise-abundant fibrosis in PDAC tumor, pancreatic tumor tissue from KPC genetic model of PDAC was evaluated by Masson-trichrome staining. We observed that DC vaccine treated KPC genetic model of PDAC had significantly decreased levels of collagen deposition throughout the pancreas compared with control mice (**Figure 4A**, **4B**).

ADC values quantified from DW-MRI correlated with the degree of tumor fibrosis in PDAC. Average ADC values for the DC vaccine treatment group were significantly increased compared with those control mice (**Figure 4C**, **4D**). ADC values also significantly correlated with the fibrosis area evaluated by histological analysis (**Figure 4E**). Taken together, these data suggest that DC vaccine treatment reshaped PDAC tumor-induced fibrosis.

DC vaccine treatment improves the outcome of standard care in a transgenic mouse model of PDAC

The impact of i.p. administration of DC vaccine treatment on overall survival was evaluated in KPC mice. We found that DC vaccine treatment caused a significant extension of survival in the transgenic model of PDAC (**Figure 5A**). No detectable side effects or weight loss were observed throughout the treatment (**Figure 5B**). Accordingly, a similar improvement in
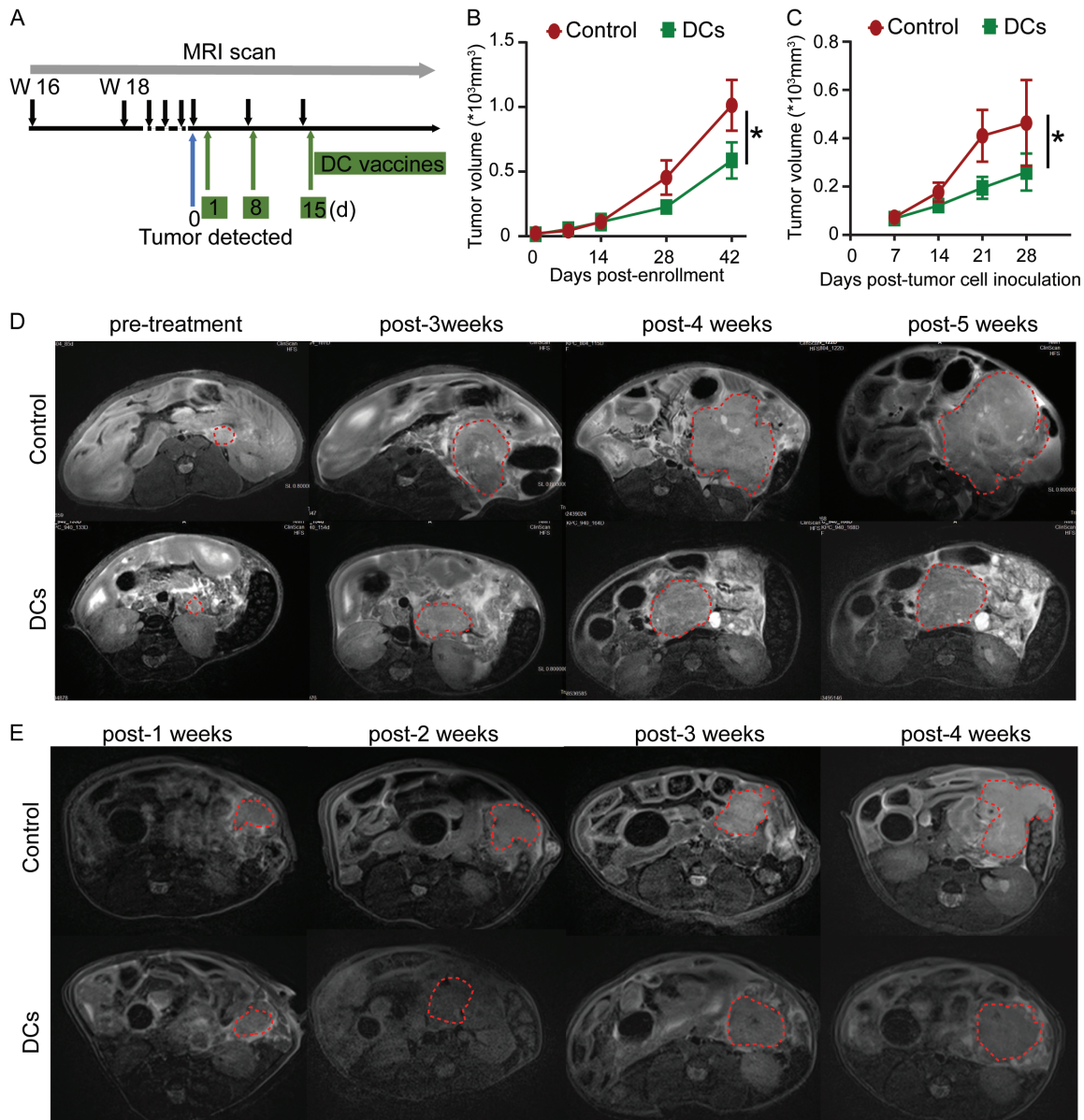
Figure 2. Vaccination with KPC pulsed DCs inhibited tumor growth in KPC mice. A. Experimental schemes for the MRI scan and treatment of the KPC genetic model. B. Measurement of tumor volumes in KPC transgenic mice (n = 7-8). C. Measurement of tumor volumes in orthotopic KPC tumor-bearing mice (n = 5). *P < 0.05. Data are expressed as the mean ± SEM. D. Representative T2W images of KPC genetic model. Red contour denotes area of pancreatic tumor. E. Representative T2W images of KPC orthotopic model. Red contour denotes area of pancreatic tumor.

survival was observed in orthotopic KPC model (**Figure 5C**), with no significant difference in mice body weight among the two groups (**Figure 5D**).

Discussion

In this study, we demonstrated that i.p. administration of DC vaccine effectively reduced

tumor volume and extended survival in highly aggressive KPC and orthotopic KPC mouse models of PDAC. The results showed that i.p. delivery of DC vaccine allowed effective migration to the dLNs, which is important for CTLs induction. Furthermore, we observed that DC vaccine treatment improved the tumor immune microenvironment of KPC, as shown by increased tumor infiltrating CD8+ CTLs and
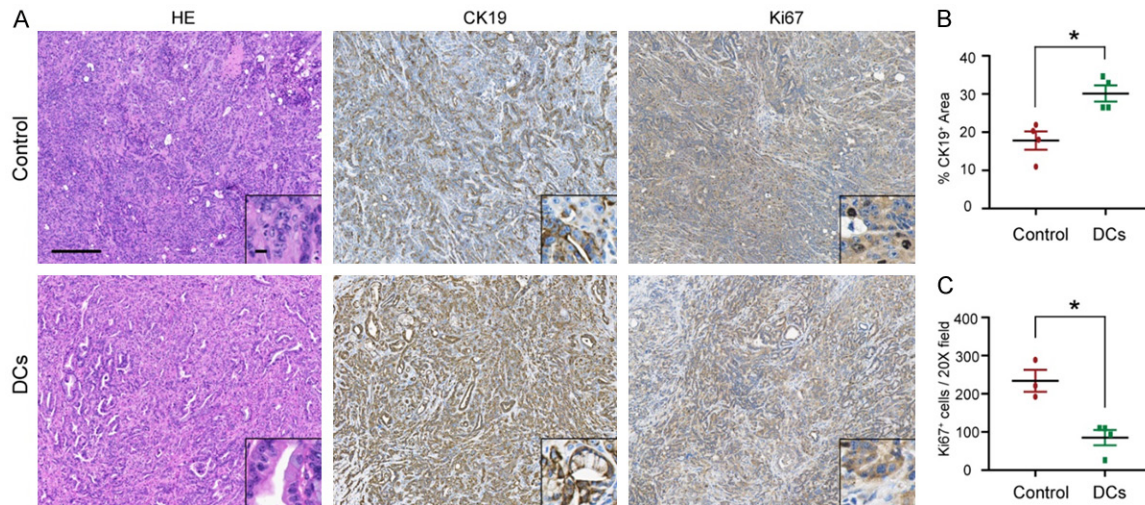
Figure 3. DC immunotherapy ameliorated pancreatic tumor progression. A. Representative images of H&E and immunohistochemical analyses in PDAC from KPC mice in treated and control groups are shown. Scale bars represent 100 μm (inset, 20 μm). B. Quantification of CK19 staining from treated and control KPC mice. C. Quantification of stromal and tumor Ki67^{+} cells from treated and control KPC mice. n = 4; *P < 0.01. Data are expressed as the mean ± SEM.
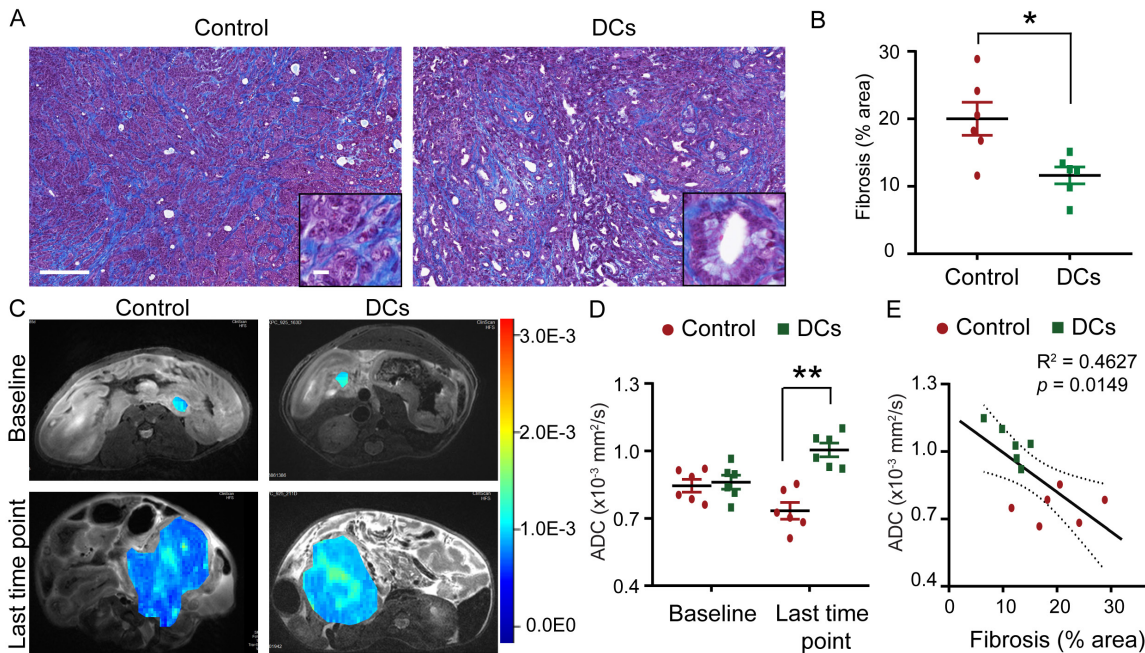

Figure 4. DC vaccine decreased fibrosis in KPC tumor. A. Representative images of trichrome staining for collagen connective tissue deposition in PDAC from treated and control KPC genetic model of PDAC. Scale bars represent 200 μm (inset, 25 μm). B. Relative quantification of collagen stained area for each group. n = 6; *P < 0.05. C. Representative ADC pseudocolor maps of the tumor overlaid onto a T2-weighted image from KPC genetic model of PDAC in treated and control cohorts are shown. D. ADC values measured from KPC genetic model of PDAC in treated and control groups at baseline and last time point. n = 6; **P < 0.001. E. Linear correlation analyses between ADC values and histology measurement of fibrosis area. R^2 = 0.46, P = 0.015. Data are expressed as the mean ± SEM.

alterations of stromal fibrosis. In addition, we also observed an inhibition of tumor growth and a significant reduction of tumor ADC values which was correlated with decreased fi-

brosis after DC vaccine treatment in KPC mice. Importantly, a significant improvement of overall survival was observed in this study. Pancreatic drawing LN metastases, liver metastases
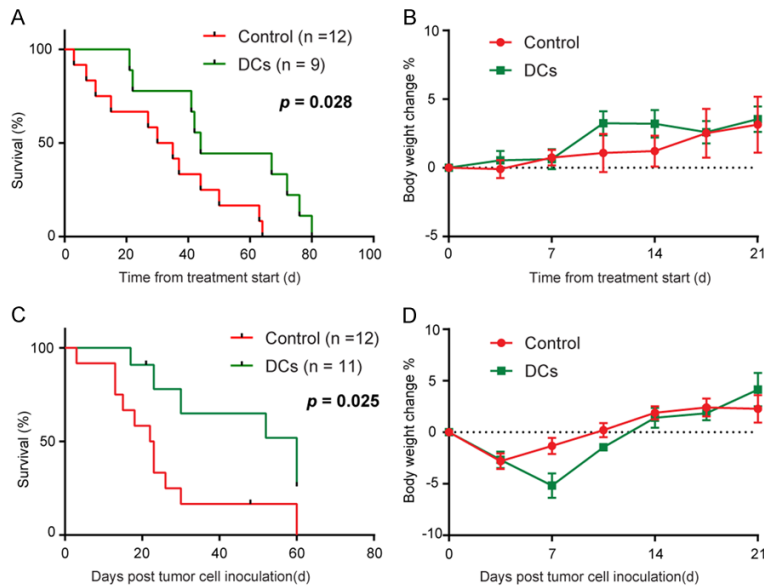
Figure 5. DC vaccine treatment has a significant therapeutic impact. A. Survival rate of treated KPC transgenic mice. Treatment start at 0.2-0.5 cm in longitudinal diameter tumor detected. DC vaccine confers survival advantage to the treated animals (P = 0.028, log-rank test). B. No significant change in the body weight of KPC transgenic mice treated with DC vaccine. Body weight was assessed twice a week and represented as percentage body weight change, mean ± SEM. C. Survival rate of treated orthotopic KPC tumor-bearing mice. Treatment start at 5 days after KPC cell inoculated. DC vaccine confers survival advantage to the treated animals (P = 0.025, log-rank test). D. No significant change in the body weight of orthotopic KPC tumor-bearing mice treated with DC vaccine. Body weight was assessed twice a week and represented as percentage body weight change, mean ± SEM.

fore incubating with DCs. UV-irradiation approach has been used in our lab with established test-retest, reliability, and reproducibility. Apoptotic PDAC cells generated by UV-B irradiation was used for DC vaccine pulsing due to its advantage in antigen loading effectiveness and the capacity of priming T-cells response [32, 33]. Therefore, in this study, we used the irradiated tumor cells for DC loading to allow the presentation of a full complement of tumor-associated antigens and induce cytotoxic responses across a broad spectrum of heterogeneous PDAC tumor cells. As with previous studies [34, 35], whole-cell-based DC vaccine can effectively induce the tumor specific cytotoxic response in PDAC.

Although previous studies have shown that DC-based immunotherapy can induce a PDAC specific immune response in clinical trials, disease progression was inevitable in almost all cases [5, 36-38]. To improve treatment efficacy of DC immunotherapy, it is probably more beneficial to enhance DC vaccine migration to the LNs. The vaccine injection site has great influence over both DC migration and antitumor response initiation [30], especially with respect to tumor localization [39]. In theory, i.p. administration may be more effective for PDAC treatment because it could accelerate DC migration to abdominal LNs. Moreover, delivering DC vaccines via an i.p. route was feasible and well tolerated. Transgenic mouse models offering an alternative to allograft and xenograft models are currently being widely used to study tumor biology, disease progression, and responses to therapy. In the KPC model of PDAC, targeted pancreatic expression of mutant *Kras* and *p53* at the endogenous loci, causing the spontaneous development of invasive and metastatic carcinoma in immune-competent hosts [40]. KPC mice with appropriately sized tumors demonstrate consistent tumor growth, which permits robust analyses for developing novel ther-

and lung metastases were observed by histological methods in our studies, but they are too small to visualize by MRI (less than 1 mm in a diameter). These metastases are defined as non-measurable lesions in MRI by RECIST (Response Evaluation Criteria in Solid Tumors) Criteria [31], therefore they are not included for analysis. In this study, we focused on primary tumor.

The selection of antigens is crucial for PDAC immunotherapy as no defined single antigen is specifically expressed in PADC cells. An alternative approach is the use of tumor lysates or tumor necrotic bodies as a source of DC loading antigens. We searched the literature and compare the UV with IR in the preparation of cancer cell for vaccine. The study conducted by Deacon et al showed that UV-irradiation can induce more significant levels of cancer cell apoptosis than IR in the preparation of cancer cell for vaccine [32]. In our previous studies (past 5 years), we have considerable experiences with UV-irradiation the cancer cells be-

apeutic approaches [29]. Thus, we utilized the KPC mice to evaluate the efficacy and therapeutic responses of the DC vaccination. Our study showed that i.p. administration of DC vaccines offers distinct advantages over current injection route for PDAC, including intratumor route and subcutaneous route [41-43]. Indeed, we observed an extend overall survival accompanied by an enhanced accumulation of tumor-infiltrating CD8+ T cells and a stronger induction of IFN-γ in KPC mice. These findings provide evidence that the improved vaccination strategy, i.p. administration of DC vaccine pulsed with irradiated tumor cells, can be a feasible and effective approach for PDAC immunotherapy and provides an avenue for future clinical studies in patients.

In PDAC, the fibrotic stromal reaction is characterized by extensive recruitment and activation of cancer associated fibroblasts and inversely correlates with patient prognosis [44-46]. Unlike targeted depletion of stromal fibroblasts in autochthonous PDAC which appeared to accelerate pancreatic cancer progression [47], the DC vaccine therapy presented here remodeled the stroma and still conferred a survival benefit. We speculate that DC vaccine treatment can reshape the fibrotic stroma, thereby allowing T-cell infiltration of tumors and improving the therapeutic effect. In this regard, further investigations on stromal contributions to DC vaccine treatment will undoubtedly inform future studies and refinements of this strategy.

Although RECIST criteria are widely used for the evaluation of therapeutic efficacy for PDAC, they may only reflect tumor response to therapy after some delay in time. An imaging biomarker that allows early assessment of response to PDAC is urgently needed. DW-MRI has the potential to detect macromolecular and microstructural changes at the cellular level prior to anatomical changes during therapy. In PDAC, a low ADC, corresponding to early progression, may be attributed to high cellularity and thus a more aggressive tumor. Several recent studies have shown that the ADC values measured from DW-MRI can serve as a potential imaging biomarker for predicting tumor response to chemotherapy for pancreatic cancer [24-26, 48]. Here, we also observed an increased ADC in KPC mice following DC vaccination. Theoretically, extracellular fibrosis characterized by extracellular accumulation of col-

lagen might influence the restriction of water diffusion, resulting in a low ADC value [49]. In our study, the ADC calculated from DW-MRI was correlated with PDAC tumor collagen content, which is in line with previous reports [50-52].

There are also limitations in this study. First, no complete tumor eradication was observed in this study. So far, there are no published studies of cures of KPC mice bearing established progressive tumors, underlining the importance of targeting PDAC immunotherapy simultaneously with multiple therapeutic options, including surgical resection, biological agents, and chemotherapeutic agents. Second, PDAC tumor microenvironment/fibrotic stroma that facilitate a paucity of infiltrating T cells need to be studied in the future. Finally, due to the mouse pancreas is considerably smaller, the ADC values were not excluded necrotic areas that might influence the results, but on T2W, no significant tumor necrotic areas were observed.

This study demonstrates that immunization with DC vaccine generated using our approach can elicit a strong antigen-specific immune response, delay tumor growth, and prolong overall survival in KPC mouse model of PDAC, and thus is the driving force to test if improved DC vaccination strategy can effectively control PDAC progression in patients.

Acknowledgements

Disclosure of conflict of interest

None.

Address correspondence to: Zhuoli Zhang, Department of Radiology, Feinberg School of Medicine, Northwestern University, 737 N Michigan Ave,

16th Floor, Chicago, IL 60611, USA. Tel: 312-695-5753; Fax: 312-926-5991; E-mail: zhuoli-zhang@northwestern.edu; Chunhong Hu, Department of Radiology, The First Affiliated Hospital of Soochow University, Suzhou 215006, Jiangsu, China. Tel: +86(512)6778-0422; E-mail: hch5305@163.com

References

[1] Siegel RL, Miller KD and Jemal A. Cancer statistics, 2018. CA Cancer J Clin 2018; 68: 7-30.

[2] Jemal A, Siegel R, Ward E, Hao Y, Xu J and Thun MJ. Cancer statistics, 2009. CA Cancer J Clin 2009; 59: 225-249.

[3] Vincent A, Herman J, Schulick R, Hruban RH and Goggins M. Pancreatic cancer. Lancet 2011; 378: 607-620.

[4] Desch AN, Randolph GJ, Murphy K, Gautier EL, Kedl RM, Lahoud MH, Caminschi I, Shortman K, Henson PM and Jakubzick CV. CD103+ pulmonary dendritic cells preferentially acquire and present apoptotic cell-associated antigen. J Exp Med 2011; 208: 1789-1797.

[5] Mehrotra S, Britten CD, Chin S, Garrett-Mayer E, Cloud CA, Li M, Scurti G, Salem ML, Nelson MH, Thomas MB, Paulos CM, Salazar AM, Nishimura MI, Rubinstein MP, Li Z and Cole DJ. Vaccination with poly(IC:LC) and peptide-pulsed autologous dendritic cells in patients with pancreatic cancer. J Hematol Oncol 2017; 10: 82.

[6] Anguille S, Smits EL, Lion E, van Tendeloo VF and Berneman ZN. Clinical use of dendritic cells for cancer therapy. Lancet Oncol 2014; 15: e257-e267.

[7] Stift A, Friedl J, Dubsky P, Bachleitner-Hofmann T, Schueller G, Zontsich T, Benkoe T, Radelbauer K, Brostjan C, Jakesz R and Gnant M. Dendritic cell-based vaccination in solid cancer. J Clin Oncol 2003; 21: 135-142.

[8] Nakamura M, Wada J, Suzuki H, Tanaka M, Katano M and Morisaki T. Long-term outcome of immunotherapy for patients with refractory pancreatic cancer. Anticancer Res 2009; 29: 831-836.

[9] Zhang Y, Ma B, Zhou Y, Zhang M, Qiu X, Sui Y, Zhang X, Ma B and Fan Q. Dendritic cells fused with allogeneic breast cancer cell line induce tumor antigen-specific CTL responses against autologous breast cancer cells. Breast Cancer Res Treat 2007; 105: 277-286.

[10] Harris RC, Chianese-Bullock KA, Petroni GR, Schaefer JT, Brill LB 2nd, Molhoek KR, Deacon DH, Patterson JW and Slingluff CL Jr. The vaccine-site microenvironment induced by injection of incomplete Freund's adjuvant, with or without melanoma peptides. J Immunother 2012; 35: 78-88.

[11] Morse MA, Deng Y, Coleman D, Hull S, Kitrell-Fisher E, Nair S, Schlom J, Ryback ME and Ly-

erly HK. A phase I study of active immunotherapy with carcinoembryonic antigen peptide (CAP-1)-pulsed, autologous human cultured dendritic cells in patients with metastatic malignancies expressing carcinoembryonic antigen. Clin Cancer Res 1999; 5: 1331-1338.

[12] Bol KF, Aarntzen EH, Pots JM, Olde Nordkamp MA, van de Rakt MW, Scharenborg NM, de Boer AJ, van Oorschot TG, Croockewit SA, Blokx WA, Oyen WJ, Boerman OC, Mus RD, van Rossum MM, van der Graaf CA, Punt CJ, Adema GJ, Figdor CG, de Vries IJ and Schreibelt G. Prophylactic vaccines are potent activators of monocyte-derived dendritic cells and drive effective anti-tumor responses in melanoma patients at the cost of toxicity. Cancer Immunol Immunother 2016; 65: 327-339.

[13] Baek S, Kim YM, Kim SB, Kim CS, Kwon SW, Kim Y, Kim H and Lee H. Therapeutic DC vaccination with IL-2 as a consolidation therapy for ovarian cancer patients: a phase I/II trial. Cell Mol Immunol 2015; 12: 87-95.

[14] Subbiah V, Murthy R, Hong DS, Prins RM, Hosing C, Hendricks K, Kolli D, Noffsinger L, Brown R, McGuire M, Fu S, Piha-Paul S, Naing A, Conley AP, Benjamin RS, Kaur I and Bosch ML. Cytokines produced by dendritic cells administered intratumorally correlate with clinical outcome in patients with diverse cancers. Clin Cancer Res 2018; 24: 3845-3856.

[15] Wang B, Sun C, Wang S, Shang N, Shangguan J, Figini M, Pan L, Zhou K, Ma Q, Procissi D, Velichko Y, Yaghmai V, Li G and Zhang Z. Mouse dendritic cell migration in abdominal lymph nodes by intraperitoneal administration. Am J Transl Res 2018; 10: 2859-2867.

[16] Wang B, Sun C, Wang S, Shang N, Figini M, Ma Q, Gu S, Procissi D, Yaghmai V, Li G, Larson A and Zhang Z. Image-guided dendritic cell-based vaccine immunotherapy in murine carcinoma models. Am J Transl Res 2017; 4564-4573.

[17] Zhang Z, Li W, Procissi D, Li K, Sheu AY, Gordon AC, Guo Y, Khazaie K, Huan Y, Han G and Larson AC. Antigen-loaded dendritic cell migration: MR imaging in a pancreatic carcinoma model. Radiology 2015; 274: 192-200.

[18] Bipat S, Phoa SS, van Delden OM, Bossuyt PM, Gouma DJ, Laméris JS, Stoker J. Ultrasonography, computed tomography and magnetic resonance imaging for diagnosis and determining resectability of pancreatic adenocarcinoma: a meta-analysis. J Comput Assist Tomogr 2005; 29: 438-445.

[19] Chandarana H, Babb J and Macari M. Signal characteristic and enhancement patterns of pancreatic adenocarcinoma: evaluation with dynamic gadolinium enhanced MRI. Clin Radiol 2007; 62: 876-883.

[20] Shami VM, Anshu Mahajan, Loch MM, Stella AC, Northup PG, White GE, Brock AS, Srinivasan I, Lange EE and Kahaleh M. Comparison between endoscopic ultrasound and magnetic resonance imaging for the staging of pancreatic cancer. Pancreas 2011; 40: 567-570.

[21] Kuroki-Suzuki S, Kuroki Y, Nasu K, Nagashima C, Machida M, Muramatsu Y and Moriyama N. Pancreatic cancer screening employing non-contrast magnetic resonance imaging combined with ultrasonography. Jpn J Radiol 2011; 29: 265-271.

[22] Bihan DL. Molecular diffusion, tissue microdynamics and microstructure. NMR Biomed 1995; 8: 375-86.

[23] Kamisawa T, Takuma K, Anjiki H, Egawa N, Hata T, Kurata M, Honda G, Tsuruta K, Suzuki M, Kamata N and Sasaki T. Differentiation of autoimmune pancreatitis from pancreatic cancer by diffusion-weighted MRI. Am J Gastroenterol 2010; 105: 1870-1875.

[24] Niwa T, Ueno M, Ohkawa S, Yoshida T, Doiuchi T, Ito K and Inoue T. Advanced pancreatic cancer: the use of the apparent diffusion coefficient to predict response to chemotherapy. Br J Radiol 2009; 82: 28-34.

[25] Cuneo KC, Chenevert TL, Ben-Josef E, Feng MU, Greenson JK, Hussain HK, Simeone DM, Schipper MJ, Anderson MA, Zalupski MM, Al-Hawary M, Galban CJ, Rehemtulla A, Feng FY, Lawrence TS and Ross BD. A pilot study of diffusion-weighted MRI in patients undergoing neoadjuvant chemoradiation for pancreatic cancer. Transl Oncol 2014; 7: 644-649.

[26] Nishiofuku H, Tanaka T, Marugami N, Sho M, Akahori T, Nakajima Y and Kichikawa K. Increased tumour ADC value during chemotherapy predicts improved survival in unresectable pancreatic cancer. Eur Radiol 2016; 26: 1835-1842.

[27] Stromnes IM, Schmitt TM, Hulbert A, Brockenbrough JS, Nguyen H, Cuevas C, Dotson AM, Tan X, Hotes JL, Greenberg PD and Hingorani SR. T cells engineered against a native antigen can surmount immunologic and physical barriers to treat pancreatic ductal adenocarcinoma. Cancer Cell 2015; 28: 638-652.

[28] Lutz M, Kukutsch N, Ogilvie A, Rössner S, Koch F, Romani N and Schuler G. An advanced culture method for generating large quantities of highly pure dendritic cells from mouse bone marrow. J Immunol Methods 1999; 223: 77-92.

[29] Hu S, Pan L, Shangguan J, Figini M, Eresen A, Sun C, Wang B, Ma Q, Hu C, Yaghmai V, Velichko Y, Yang J and Zhang Z. Non-invasive dynamic monitoring initiation and growth of pancreatic tumor in the LSL-Kras(G12D/+);LSL-Trp53(R172H/+);Pdx-1-Cre (KPC) transgenic mouse model. J Immunol Methods 2019; 465: 1-6.

[30] Mullins DW, Sheasley SL, Ream RM, Bullock TN, Fu YX and Engelhard VH. Route of immunization with peptide-pulsed dendritic cells controls the distribution of memory and effector T cells in lymphoid tissues and determines the pattern of regional tumor control. J Exp Med 2003; 198: 1023-1034.

[31] Eisenhauer EA, Therasse P, Bogaerts J, Schwartz LH, Sargent D, Ford R, Dancey J, Arbuck S, Gwyther S, Mooney M, Rubinstein L, Shankar L, Dodd L, Kaplan R, Lacombe D and Verweij J. New response evaluation criteria in solid tumours: revised RECIST guideline (version 1.1). Eur J Cancer 2009; 45: 228-247.

[32] Deacon DH, Hogan KT, Swanson EM, Chianese-Bullock KA, Denlinger CE, Czarkowski AR, Schrecengost RS, Patterson JW, Teague MW and Slingluff CL Jr. The use of gamma-irradiation and ultraviolet-irradiation in the preparation of human melanoma cells for use in autologous whole-cell vaccines. BMC Cancer 2008; 8: 360.

[33] Inzkirweli N, Gückel B, Sohn C, Wallwiener D, Bastert G and Lindner M. Antigen loading of dendritic cells with apoptotic tumor cell-preparations is superior to that using necrotic cells or tumor lysates. Anticancer Res 2007; 27: 2121-2130.

[34] Konduri V, Li D, Halpert MM, Liang D, Liang Z, Chen Y, Fisher WE, Paust S, Levitt JM, Yao QC and Decker WK. Chemo-immunotherapy mediates durable cure of orthotopic Kras(G12D)/p53(-/-) pancreatic ductal adenocarcinoma. Oncoimmunology 2016; 5: e1213933.

[35] Kim HS, Choo YS, Koo T, Bang S, Oh TY, Wen J and Song SY. Enhancement of antitumor immunity of dendritic cells pulsed with heat-treated tumor lysate in murine pancreatic cancer. Immunol Lett 2006; 103: 142-148.

[36] Collignon A, Perles-Barbacaru AT, Robert S, Silvy F, Martinez E, Viola A, Crenon I, Germain S, Garcia S, Viola A, Lombardo D, Mas E and Béraud E. A pancreatic tumor-specific biomarker characterized in humans and mice as an immunogenic onco-glycoprotein is efficient in dendritic cell vaccination. Oncotarget 2015; 6: 23462-23479.

[37] Takakura K, Koido S, Kan S, Yoshida K, Mori M, Hirano Y, Ito Z, Kobayashi H, Takami S, Matsumoto Y, Kajihara M, Misawa T, Okamoto M, Sugiyama H, Homma S, Ohkusa T and Tajiri H. Prognostic markers for patient outcome following vaccination with multiple MHC Class I II-restricted WT1 peptide-pulsed dendritic cells plus chemotherapy for pancreatic cancer. Anticancer Res 2015; 35: 555-562.

[38] Yanagisawa R, Koizumi T, Koya T, Sano K, Koido S, Nagai K, Kobayashi M, Okamoto M, Sugi-

yama H and Shimodaira S. WT1-pulsed dendritic cell vaccine combined with chemotherapy for resected pancreatic cancer in a phase I study. Anticancer Res 2018; 38: 2217-2225.

[39] Ohlfest JR, Andersen BM, Litterman AJ, Xia J, Pennell CA, Swier LE, Salazar AM and Olin MR. Vaccine injection site matters: qualitative and quantitative defects in CD8 T cells primed as a function of proximity to the tumor in a murine glioma model. J Immunol 2013; 190: 613-620.

[40] Hingorani SR, Wang L, Multani AS, Combs C, Deramaudt TB, Hruban RH, Rustgi AK, Chang S and Tuveson DA. Trp53R172H and Kras-G12D cooperate to promote chromosomal instability and widely metastatic pancreatic ductal adenocarcinoma in mice. Cancer Cell 2005; 7: 469-483.

[41] Bauer C, Bauernfeind F, Sterzik A, Orban M, Schnurr M, Lehr HA, Endres S, Eigler A and Dauer M. Dendritic cell-based vaccination combined with gemcitabine increases survival in a murine pancreatic carcinoma model. Gut 2007; 56: 1275-1282.

[42] Schmidt T, Ziske C, Märten A, Endres S, Tiemann K, Schmitz V, Gorschlüter M, Schneider C, Sauerbruch T, Schmidt-Wolf IG. Intratumoral immunization with tumor RNA-pulsed dendritic cells confers antitumor immunity in a C57BL 6 pancreatic murine tumor model. Cancer Res 2003; 8962-8967.

[43] Nagaraj S, Ziske C, Strehl J, Messmer D, Sauerbruch T and Schmidt-Wolf IG. Dendritic cells pulsed with alpha-galactosylceramide induce anti-tumor immunity against pancreatic cancer in vivo. Int Immunol 2006; 18: 1279-1283.

[44] Whatcott CJ, Diep CH, Jiang P, Watanabe A, LoBello J, Sima C, Hostetter G, Shepard HM, Von Hoff DD and Han H. Desmoplasia in primary tumors and metastatic lesions of pancreatic cancer. Clin Cancer Res 2015; 21: 3561-3568.

[45] Sinha S and Leach SD. New insights in the development of pancreatic cancer. Curr Opin Gastroenterol 2016; 32: 394-400.

[46] Kleeff J, Korc M, Apte M, La Vecchia C, Johnson CD, Biankin AV, Neale RE, Tempero M, Tuveson DA, Hruban RH and Neoptolemos JP. Pancreatic cancer. Nat Rev Dis Primers 2016; 2: 16022.

[47] Ozdemir BC, Pentcheva-Hoang T, Carstens JL, Zheng X, Wu CC, Simpson TR, Laklai H, Sugimoto H, Kahlert C, Novitskiy SV, De Jesus-Acosta A, Sharma P, Heidari P, Mahmood U, Chin L, Moses HL, Weaver VM, Maitra A, Allison JP, LeBleu VS and Kalluri R. Depletion of carcinoma-associated fibroblasts and fibrosis induces immunosuppression and accelerates pancreas cancer with reduced survival. Cancer Cell 2014; 25: 719-734.

[48] Okada KI, Hirono S, Kawai M, Miyazawa M, Shimizu A, Kitahata Y, Ueno M, Hayami S, Kojima F and Yamaue H. Value of apparent diffusion coefficient prior to neoadjuvant therapy is a predictor of histologic response in patients with borderline resectable pancreatic carcinoma. J Hepatobiliary Pancreat Sci 2017; 24: 161-168.

[49] Bihan DL, Breton E, Lallemand D, Aubin ML, Vignaud J and Laval-Jeantet M. Separation of diffusion and perfusion in intravoxel incoherent motion MR imaging. Radiology 1988; 168: 497-505.

[50] Wegner CS, Hauge A, Gaustad JV, Andersen LMK, Simonsen TG, Galappathi K and Rofstad EK. Dynamic contrast-enhanced MRI of the microenvironment of pancreatic adenocarcinoma xenografts. Acta Oncol 2017; 56: 1754-1762.

[51] Chen BB, Tien YW, Chang MC, Cheng MF, Chang YT, Yang SH, Wu CH, Kuo TC, Shih IL, Yen RF and Shih TT. Multiparametric PET/MR imaging biomarkers are associated with overall survival in patients with pancreatic cancer. Eur J Nucl Med Mol Imaging 2018; 45: 1205-1217.

[52] Chen BB, Tien YW, Chang MC, Cheng MF, Chang YT, Wu CH, Chen XJ, Kuo TC, Yang SH, Shih IL, Lai HS and Shih TT. PET/MRI in pancreatic and periampullary cancer: correlating diffusion-weighted imaging, MR spectroscopy and glucose metabolic activity with clinical stage and prognosis. Eur J Nucl Med Mol Imaging 2016; 43: 1753-1764.
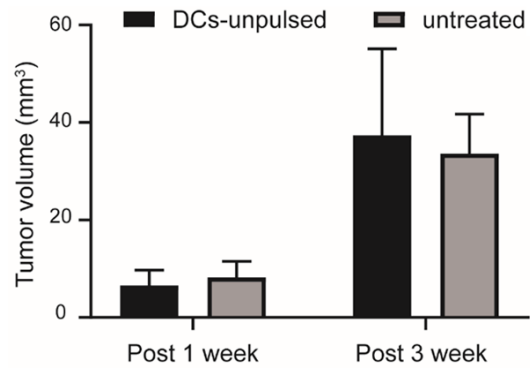
Figure S1. Measurement of tumor volumes in orthotopic PDAC mice (n = 4). P = 0.916. Data are expressed as the mean ± SEM. Statistical analysis was performed by using one-way ANOVA.